DYCOMS-II

Bjorn Stevens, Donald H. Lenschow and Verica Savic-Jovcic

5th August 2001

1 Overview

DYCOMS-II took place in the general vicinity of 122° W 31° N over a three week period with three flights per week as indicated in Table 1. The synoptic conditions during the first and third weeks were most similar. For both of these weeks the surface high tended to have a somewhat NW-SE orientation, with surface isobars moving offshore somewhere between Portland and Point Conception. Under these conditions the 850 hPa temperatures tended to largest, reflecting more continental conditions. Concurrently the cloud layer tended to be shallower, generally under 850m, with relatively little evolution of cloud top height during the course of any given flight.

Table 1: DYCOMS II research flights. Start and end times in UTC (DD.MM.YY HHMMSS format).

Flight	Start	End	Type
RF01	07.10.2001 060059	07.10.2001 151813	Entrainment
RF02	07.11.2001 062440	07.11.2001 155235	Entrainment
RF03	07.13.2001 061823	07.13.2001 154603	Entrainment
RF04	07.17.2001 062238	07.17.2001 153130	Entrainment
RF05	07.18.2001 061847	07.18.2001 154057	Entrainment
RF06	07.20.2001 053944	07.20.2001 151300	Radar
RF07	07.24.2001 055322	07.24.2001 154919	Entrainment
RF08	07.26.2001 194522	07.27.2001 052034	Entrainment
RF09	07.27.2001 181558	07.28.2001 034515	Radar

At the end of the first week the surface high strengthened and became oriented in a more north-south direction. At the same time a strong low pressure system developed off the coast of British Columbia, and was centered over Seattle at 00Z on the 17th. The influence of this depression was felt over the target area at upper levels and was associated with strong cold advection aloft. The 850 hPa temperatures decreased from 4-8K resulting in significantly weaker inversions and generally deeper (800-1100m) boundary layers which displayed more evolution in cloud top height through the course of a given mission.

Analyses of sea surface temperatures by the Naval Oceanographic office estimated SSTs of 18-22° C over the target area. At the beginning of the experiment SST gradients in the target area tended to be primarily North-South. Toward the middle of the first week a warm anomaly is evident in the SW corner of the general target area. After this change SSTs tended to be 1-3° warmer in the SW corner of the $2 \times 2°$ box whose NW corner was at 32N and 122W.

Back trajectories tended to vary little from flight to flight. For parcels on target at 1500m appeared to have originated at higher elevations (typically 3000m) somewhere North or North-West of the target. RF03 and RF01 were exceptions, back trajectories of air aloft suggest a more westerly origin. In the boundary layer (at 250m) back trajectories generally indicated marine origins. For the most part the trajectories remained in the boundary layer as they were tracked back in time. RF03 was again an exception, its back trajectory was analyzed to have been over Northwest Oregon three days prior to the flight.

Microphysically the clouds varied less systematically with the macroscopic conditions. For instance although RF01-RF03 took place in similar synoptic conditions drizzle was relatively unimportant in RF01, strong in RF01 and modest in RF03. Overall drizzle was most prevalent in RF02, but was also evident in RF04, RF06 and RF07. In RF04 which had a relatively weak drizzle signature liquid water mixing-ratios were over 0.8 gkg^{-1} at cloud top, whereas there was pronounced drizzle during RF02 where liquid water mixing-ratios had maxima closer to 0.5 gkg^{-1}. Overall the maximum liquid water mixing-ratios in the cloud layer varied more than two fold, from a minimum of 0.3 during RF05 to maxima greater than 0.8 on RF04 and RF07. All of the cases had solid cloud cover, with only RF02 having cloud fractions (as determined by the fraction of time the lidar showed returns from the surface) less than one. Cloud fraction during RF02 was 97 %.

There was also considerable variation in the chemical structure of the atmosphere that also did not strongly correlate with the week to week synoptic variability. CCN (at 1%) concentrations varied substantially from a minimum of about 60 to a maximum of near 300 # cm^{-3}. Ozone concentrations and jumps also seemed to vary in an apparently more random fashion from flight to flight.

2 Research Flights

The experiment consisted of two basic flight patterns: entrainment and radar flight patterns. The entrainment flight patterns had a three-fold objective: to measure divergence and turbulent fluxes at various levels as well as characterize the mean states of both the boundary layer and the overlying air column. To achieve these objectives the basic entrainment flight plan consisted of stacks of 30 minute (approximately 60km diameter) circles. In contrast the objectives of the radar flights was to characterize the evolution of a specific convective cell. For this reason the radar flights consisted of shorter (6 minute) legs that attempted to fly over or through a specific point in the flow along varied headings.

These differences between the two flight patterns are shown in Fig. 1 which shows the flight tracks from RF08 and RF09. There were only two radar flights, RF09 and RF06, and although the flight tracks were not identical between the two, the idea was similar. The general nature of all the entrainment flights was identical, the only difference being in the ordering of the legs, and how transitions between circles were made. In general two opposing circles were flown consecutively at each altitude, thus yielding an hour at any given level. On some flights however, either the subcloud or surface layer circles were performed in only one direction in order to make time for other maneuvers. In addition the entrainment flights allowed time for one leg whose objective was determined on a flight by flight basis. After the second flight this leg was always a porpoising leg through the cloud top. Lastly, flight maneuvers were performed twice during the experiment. Once on the third test flight, which took place on station during the day on July 7, 2001, and once on the outbound Ferry of RF07.

Because the basic flight plan for the entrainment flights was so similar it proves useful to name

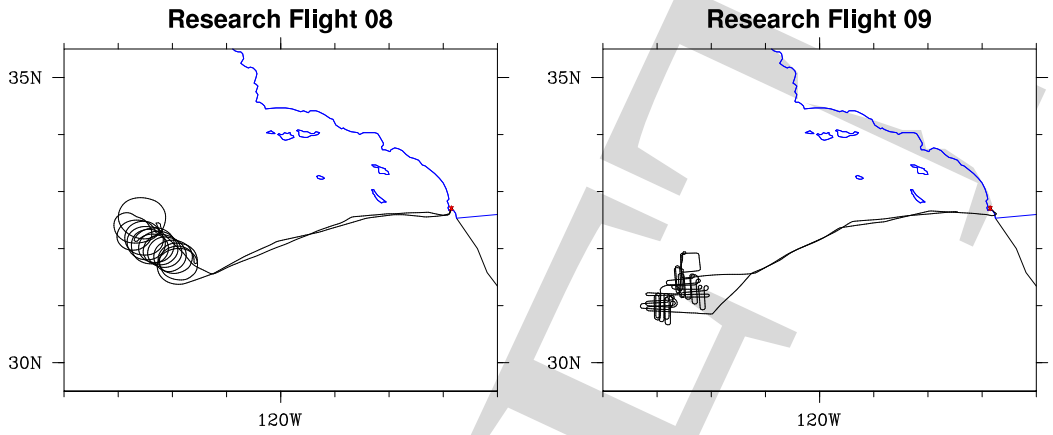

Figure 1: Flight tracks for RF08 and RF09.

Table 2: Nomenclature for entrainment flight segments.

Name	Leg or Sounding Type	Comment
RL	Radar Leg	at least 300m above cloud top
CT	Cloud top flux leg	in cloud near top
CB	Cloud base flux leg	in cloud near base
SC	Subcloud flux leg	just below cloud base
SF	Surface leg	lowest safe flight level
SP	Special leg	after RF02 a porpoising leg
FP	Full sounding	lowest safe flight level to above cloud
CP	Cloud profile	sounding of most of cloud layer
IP	Inversion profile	sounding through cloud top

various flight segments and tabulate the time-offsets[1] corresponding to each of these segments. The basic nomenclature for this segmentation is introduced in Table 2 and will be adhered to throughout. Note that two basic types of flight segments are present, soundings and level legs. The level legs are for estimating fluxes, each has been checked for constancy of altitude over the time period, but has yet to be checked for bank-angle or other anomalies. For the radar flight we only anticipate identifying sounding legs.

2.1 RF01 (07/10/2001 06:00:59-15:18:13 UTC)

Fig. 2 illustrates the mean cloud cover in the vicinity of the target area, and the mean state of the boundary layer as determined by the dropsondes. The satellite image is taken from channel 1 of the GOES 10 satellite at 1400 (UTC), and thus corresponds to a period near the end of the time at the target. The sondes are from two periods, the first being a radar leg when we first arrived at the target area, the second being from a period 5-6 hours later during the last radar leg before leaving the target area. This pattern of dropping sondes on the first and last radar legs was adhered to on all entrainment flights.

Overall the boundary layer cloud field appeared very homogeneous even down to relatively fine scales. Lidar deduced cloud cover on the last leg was unity. The dropsondes indicate that the mixed

[1] Denoted by the variable *Time offset* in the NIMBUS netCDF format.

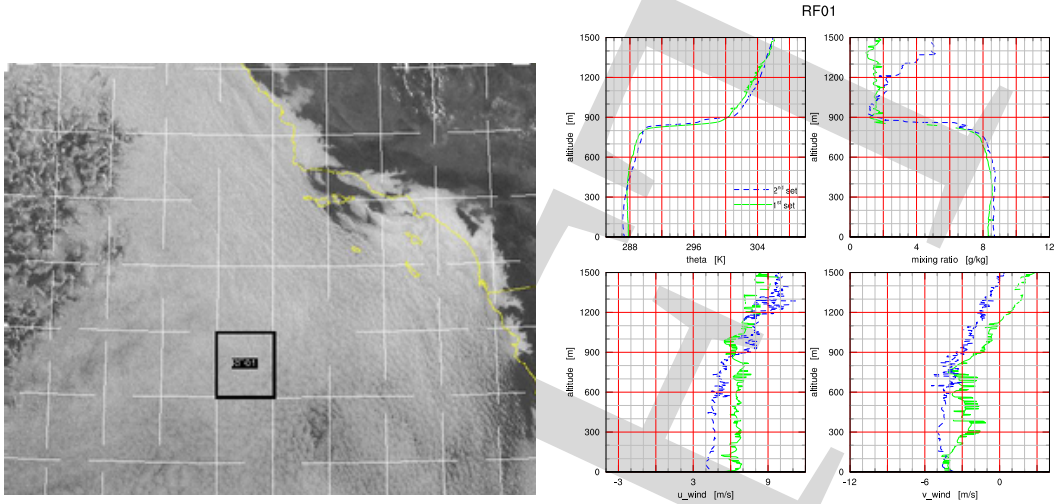

Figure 2: 1400 (UTC) cloud cover over target area and composite dropsonde data for RF01.

layer was about 850m deep and showed evidence of cooling and moistening, with only marginal deepening through the course of the flight. Cloud depth increased commensurately during the flight with liquid water mixing ratios increasing to about 0.45 gkg^{-1} at cloud top in the latter soundings. Consistent with this deepening radar echo's increased through the course of the flight. Cloud drop number concentrations were about 150 # cm^{-3}, CN concentrations were about 250 # cm^{-3} in the boundary layer, increasing to 350 # cm^{-3} aloft. There was little clear evidence of elevated haze layers.

Table 3: RF01 offset times for flight segments

#	*GALT* [m]	*Time* [s]	Type	#	*GALT* [m]	*Time* [s]	Type
1	3248 ± 3.7	5550 - 7450	RL	1	3246 - 183	7490 - 8005	FP
2	625 ± 4.2	8400 -10200	CB	2	183 - 643	8005 - 8110	FP
3	637 ± 3.5	10500 -12200	CB	3	616 - 892	10233 -10310	CP
4	487 ± 6.5	12400 -16200	SC	4	892 - 615	10310 -10426	CP
5	758 ± 3.3	16600 -18200	CT	5	494 - 915	16210 -16327	CP
6	755 ± 3.2	18500 -20100	CT	6	915 - 750	16327 -16393	CP
7	1056 ± 2.9	20700 -22400	RL	7	750 - 166	20155 -20419	CP
8	924 ± 7.0	22650 -22950	SP	8	166 - 1074	20419 -20584	FP
9	152 ± 4.2	23300 -25100	SF	9	1050 - 761	22465 -22544	IP
10	96 ± 6.4	25200 -27000	SF	10	761 - 945	22544 -22608	IP
11	1893 ± 3.2	27400 -29200	RL	11	935 - 149	22955 -23168	FP
				12	113 - 1920	27060 -27300	FP

Donald Lenschow was the flight scientist and Bjorn Stevens flew as a mission specialist. Offset times are tabulated in Table 2.1. In contrast to the flights after RF02 headings were reversed upon completion of a circle. The one non-standard leg flow was a very short, 5 minute leg, just above the highest cloud tops. This

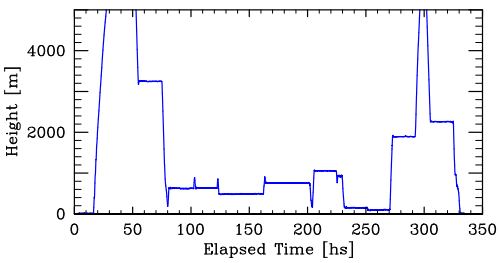

Figure 3: RF01 Flight Legs

leg appaears to have penetrated a region of boundary layer modified air in its latter half, but overall could be useful in evaluating the radiative budget in the near cloud top vicinity. Lastly, because of one circle being flown in the wrong sense, early in the time at target the aircraft moved off its initial air-mass to one 60km downstream. The homogeneity observed during the experiment suggests that this should not be a big problem.

In terms of instruments the TDL flew at 2 Hz (averaging approximately four scans per half second). The CVI did not fly because of a disk failure. The Gerber probe was connected improperly and appeared to only be getting data from one channel, which fortunately appeared to be the liquid water signal. The second radar/lidar leg was flown at an altitude below the lidar dead-zone making the lidar data of questionable use for this leg. MCR data was not available from channel 7 and thus only available for the return ferry. Initial looks at state variables showed good correspondence between lyman-alpha's below cloud, but not in cloud. Attempts to correlate the lyman-alpha with temperature in cloud, assuming that they should follow a saturation relation, failed, with early indications being that the problem was with the lyman-alphas.

2.2 RF02 (07/11/2001 06:24:40-15:52:35 UTC)

The cloud cover and dropsonde derived basic state for RF02 are displayed in Fig. 4. The stratus layer remained well formed and about the same depth as for the previous night, although the region of more distinctly cellular structure had moved toward the target area, with evidence of open celled structures in the target area itself. The lidar derived cloud fraction was still very high, 97% thus suggesting that the big regions of clearing evident in the satellite image were not present along the flight track. There was also little visual evidence of distinct breaks during the flight itself, although the cloud layer was thin enough for the moon to clearly shine through in many places — and these might have shown up as clearings in the satellite imagery. The more cellular like structure of RF02 was accompanied by pronounced drizzle. The aircraft windshield wetted, and the radar revealed pronounced drizzle echoes with returns greater than 20 dBz in the cloud, and greater than 0 dBz at the surface. Associated with distinct drizzling cells was a strong modulation of cloud top height.

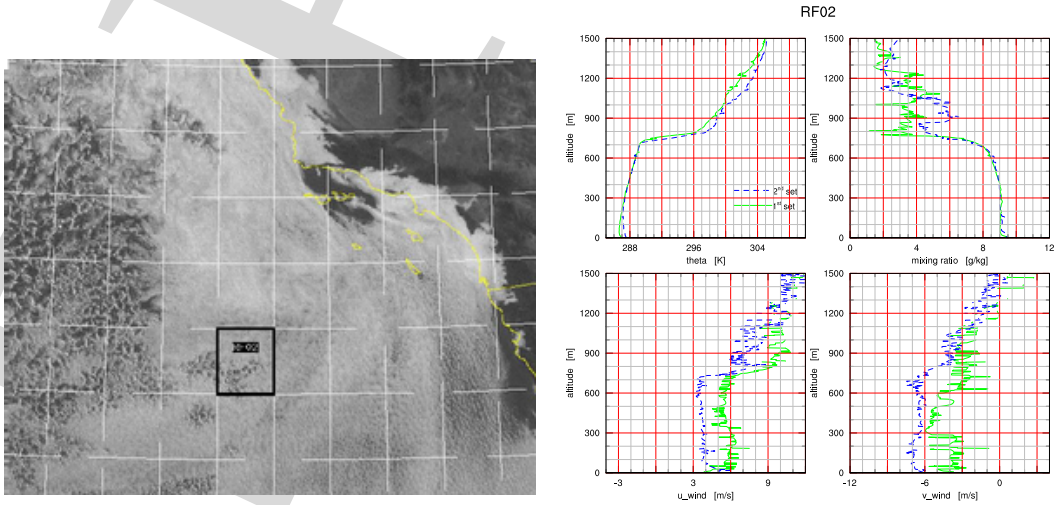

Figure 4: 1400 (UTC) cloud cover over target area and composite dropsonde data for RF02.

From the dropsonde data we note that the mixed layer shows evidence of shallowing approximately 100m from the previous day. Winds in the boundary layer tended to be of commensurate magnitude, but perhaps a bit more northerly than they were during RF01. Thermodynamically there was less evidence of changes in temperature and humidity through the course of the flight. Relative to RF01, Theta at 900m had increased approximately 2 K and the free tropospheric humidity structure was moister and significantly more variable in RF02. Ozone concentrations were also significantly reduced both in and above the boundary layer.

Although not shown, the cloud layer had more variable depth with liquid water mixing ratios peaking near 0.6 gkg^{-1} in some regions. Cloud depths, however were not significantly deeper than the previous nights. Drop concentrations were significantly reduced, with values of 50-100 drops/cc. CN and CCN concentrations above the boundary layer were commensurate with values from RF01 although both were significantly reduced in the boundary layer.

Table 4: RF02 offset times for flight segments

#	*GALT* [m]	*Time* [s]	Type	#	*GALT* [m]	*Time* [s]	Type
1	2598 ± 4.1	5520 - 7495	RL	1	2601 - 194	7502 - 8013	FP
2	485 ± 3.9	8900 -11180	CB	2	194 - 817	8013 - 8151	FP
3	517 ± 3.2	11260 -12380	CB	3	765 - 431	8349 - 8471	CP
4	271 ± 4.3	12860 -16640	SC	4	520 - 757	12422 -12470	CP
5	674 ± 4.0	16975 -20840	CT	5	758 - 198	12469 -12608	FP
6	1117 ± 3.8	21560 -23120	RL	6	166 - 790	16750 -16854	FP
7	761 ± 4.6	23300 -25100	SP	7	678 - 181	20841 -21020	FP
8	107 ± 5.1	25500 -27440	SF	8	838 - 84	25177 -25468	FP
9	2530 ± 3.0	27860 -29660	RL	9	102 -2494	27479 -27804	FP

Donald Lenschow again served as mission scientist and Bjorn Stevens flew as a mission specialist. The flight tracks were similar (cf., Fig. 5), with the offset times of the various legs again tabulated in Table 2.2. For RF02 the non-standard leg (starting at 23300 s) was a full 30 min circle at a level that tried to be at the mean cloud top height, thereby skimming in and out of cloud tops. Preliminary analysis of this leg indicated regions where the plane flew through cloud-free boundary layer air, above lower lying (perhaps reforming or decaying) cloud tops. The surface leg was shortened to 30 minutes to allow time to perform a full non-standard leg.

In terms of instruments, the TDL flew at three grab samples per second. The CVI still did not fly because of hard-ware problems. The Gerber probe was functioning properly but only at 250 Hz. The second radar/lidar leg was flown at an altitude above the lidar dead-zone, making it useful as a lidar leg

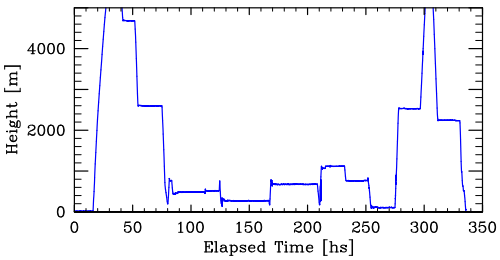

Figure 5: RF01 Flight legs

2.3 RF03 (07/13/2001 06:18:23-15:46:03 UTC)

RF03 was our Friday the 13th flight (UTC). The stratus layer again remained well formed. Relative to RF02 the satellite imagery (Fig. 6) indicated less larger-scale cellular structure near the target area. There is even

some evidence of more elongated features in the cloud field consistent with significantly stronger winds out of the north. One distinguishing feature of this flight was that back trajectories of boundary layer air indicated it was in the boundary layer in the vicinity of Portland three days previously. Another is the presence of a weak mid level disturbance whose influence is evident in the high cloud field of the satellite imagery. The winds during RF03 were the strongest (about 11 ms^{-1}) observed during the experiment. In other respects RF03 was intermediate between RF02 and RF01, with some of drizzle, but echoes at the surface tending to be less significant. The free-troposphere was more variable, as in RF02, but cloud top was more regular. Again we found deep solid cloud cover with liquid water mixing-ratios of 0.6 gkg^{-1} at cloud top, albeit in a somewhat shallower boundary layer.

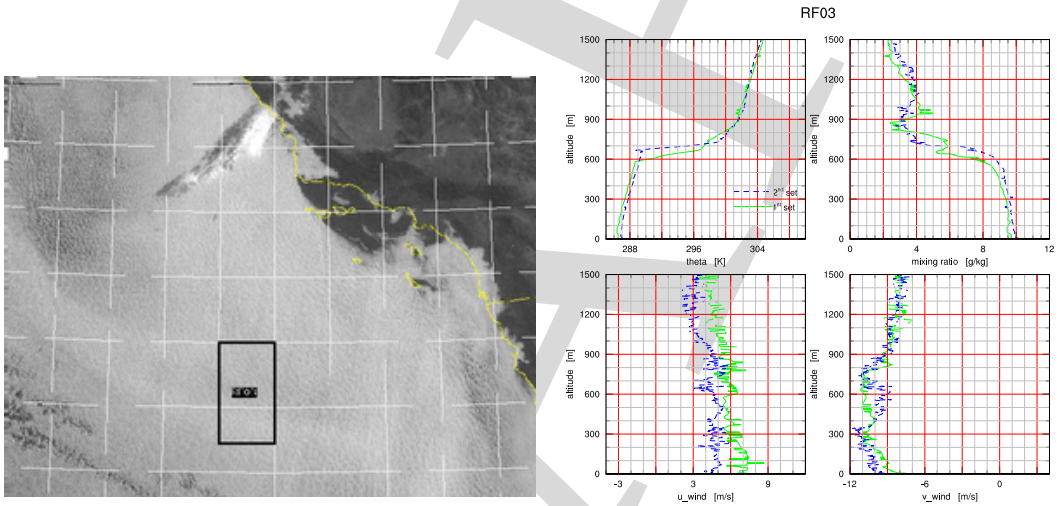

Figure 6: 1400 (UTC) cloud cover over target area and composite dropsonde data for RF03.

Table 5: RF03 offset times for flight segments

#	*GALT* [m]	*Time* [s]	Type	#	*GALT* [m]	*Time* [s]	Type
1	2620 ± 8.4	2130 - 2860	RL	1	2612 - 164	7033 - 7455	FP
2	2613 ± 3.3	3140 - 6940	RL	2	164 - 414	7455 - 7532	SP
3	377 ± 4.8	7657 -11192	CB	3	378 - 735	11247 -11317	CP
4	192 ± 4.4	11462 -13332	SC	4	735 - 176	11317 -11452	FP
5	527 ± 4.2	13537 -17262	CT	5	194 - 743	13332 -13445	FP
6	1092 ± 2.4	17723 -19523	RL	6	743 - 516	13445 -13531	CP
7	370 ± 4.3	21702 -23792	SC	7	527 - 168	17315 -17425	FP
8	98 ± 4.3	24107 -27657	SF	8	162 -1118	17450 -17603	FP
9	2547 ± 3.6	28012 -29898	RL	9	1093 - 561	19573 -19743	FP
				10	687 - 233	21454 -21662	FP
				11	233 - 179	21662 -21705	SP
				12	370 - 80	23782 -23880	SP
				13	104 -2516	27710 -27992	FP

Bjorn Stevens served as mission scientist and Don Lenschow flew as a mission specialist. The flight tracks were similar (cf., Fig. 7), with the offset times of the various legs again tabulated in Table 2.3. For RF03 the non-standard leg was a porpoising leg in and out of cloud top. We

retained this format for subsequent flights. In this flight the second circle in the subcloud layer was sacrificed for an additional half hour at cloud base toward the end of the time at target. This change allowed for evaluation of cloud evolution through the course of the experiment. The strong winds were also blowing the target area into Mexican airspace, and as a result the air mass was not exactly tracked for the entire experiment.

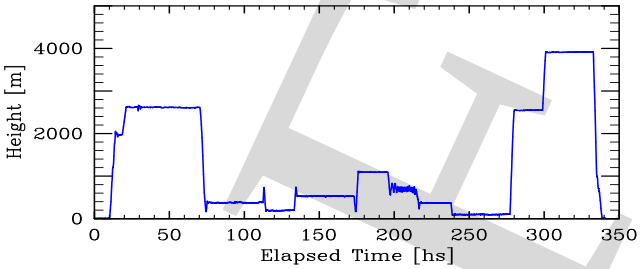

Figure 7: RF03 Flight legs

The CVI flew for the first time on this flight, and collected data. Also the UFT was up and running for most of the flight and collected good data on the porpoising leg.

2.4 RF04 07/17/2001 (06:22:38-15:31:30)

RF04 was the first flight of the second week. Over the prior weekend the marine layer had significantly weakened in association with a weakening inversion due to cold air advection aloft. Nonetheless in the vicinity of the target the stratus was again well formed. North of the target area there is evidence of cloud streaks, but clouds had a more cellular structure over the target (Fig.,6). Winds were modest from the NNW. The boundary layer cloud fraction from the last radar leg was again unity.

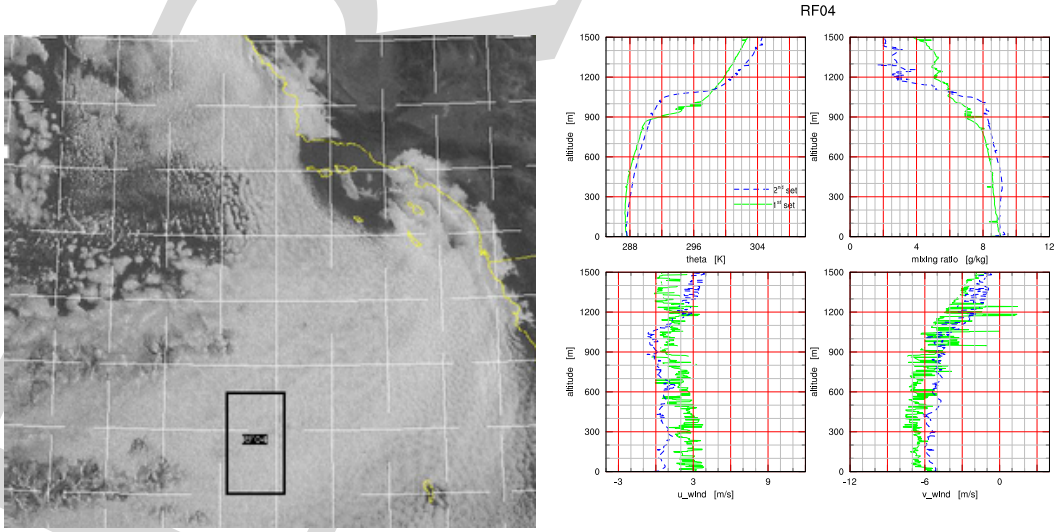

Figure 8: 1400 (UTC) cloud cover over target area and composite dropsonde data for RF04.

Distinguishing features of RF04 were its very deep boundary layer, large CCN concentrations and smaller radar echoes. In addition there is evidence of significant boundary layer deepening

through the night, as well as evolution of the flow aloft over the course of the flight. The cloud depth approached 600m with liquid water mixing ratios at cloud top well over 0.8 gkg^{-1}, reaching nearly 1 gkg^{-1} in places. Through the course of the night the dropsonde data indicates a 150-200 m deepening of the boundary layer, and at the same time the free troposphere warmed by 2K and moistened by 2 gkg^{-1}. The drying aloft and the abundance of CCN, making for smaller cloud drops, might both have contributed to the relatively small radar-echoes seen on this flight.

Table 6: RF04 offset times for flight segments

#	*GALT* [m]	*Time* [s]	Type	#	*GALT* [m]	*Time* [s]	Type
1	2582 ± 4.2	4682 - 6757	RL	1	2549 - 183	6770 - 7395	FP
2	677 ± 4.8	7807 - 11850	CB	2	183 - 1026	7395 - 7705	FP
3	369 ± 4.4	12347 - 16047	SC	3	1027 - 683	7703 - 7814	CP
4	1304 ± 2.7	16562 - 18172	RL	4	679 - 1115	11844 - 11940	CP
5	948 ± 3.4	18337 - 22072	CT	5	1115 - 181	11940 - 12250	FP
6	Porpoising	22132 - 23797	SP	6	170 - 1218	16097 - 16362	FP
7	101 ± 3.6	24172 - 26342	SF	7	1301 - 933	18174 - 18326	IP
8	2518 ± 4.3	26712 - 28547	RL	8	1135 - 99	23750 - 24150	FP
				9	105 - 2560	26345 - 26685	FP

Don Lenschow served as mission scientist, Bjorn Stevens was the mission specialist and Chris Bretherton flew as an observer. To allow time for a full porpoising leg the surface leg was flow only for one 30 minute circle. In addition, beginning with this flight the cloud top leg was flown after the second radar leg rather than before. This gave more spacing between the cloud legs and allowed the second radar leg to be more centered in time. The Gerber probe suffered from a corroded board on this flight and faded toward the end of the flight. The FSSP-100 functioned only intermittently.

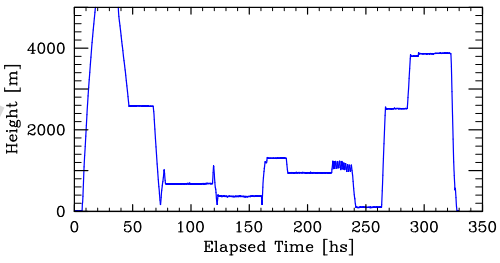

Figure 9: RF04 Flight legs

2.5 RF05 07/18/2001 (06:18:47-15:40:57 UTC)

The large scale conditions of RF04 continued during RF05, however the cloud layer did show evidence of considerable thinning and the marine layer as a whole dried. This was one of the driest flights, with liquid-water mixing ratios of only about 0.3 gkg^{-1} at cloud top and little evidence of drizzle. Still the satellite imagery (Fig. 10) shows a well formed morning cloud layer, with some evidence of larger-scale cellular structures. The sounding data indicates that similar to RF04 the boundary layer deepened significantly through the course of the flight. The free troposphere also appeared somewhat more steady during the course of the flight, with somewhat drier air aloft relative to RF05. Similar to RF05 the boundary layer cooled slightly and moistened as it deepened.

Chris Bretherton served as mission scientist, Don Lenschow was mission specialist and Verica Savic-Jovcic was an observer. The flight pattern did not depart substantially from previous flights except that the surface leg was shortened to allow additional time at

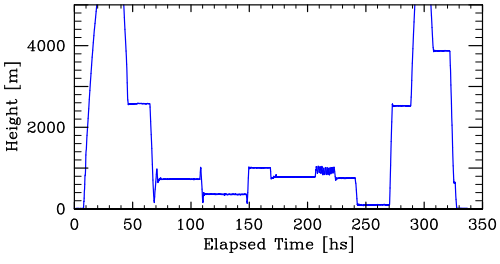

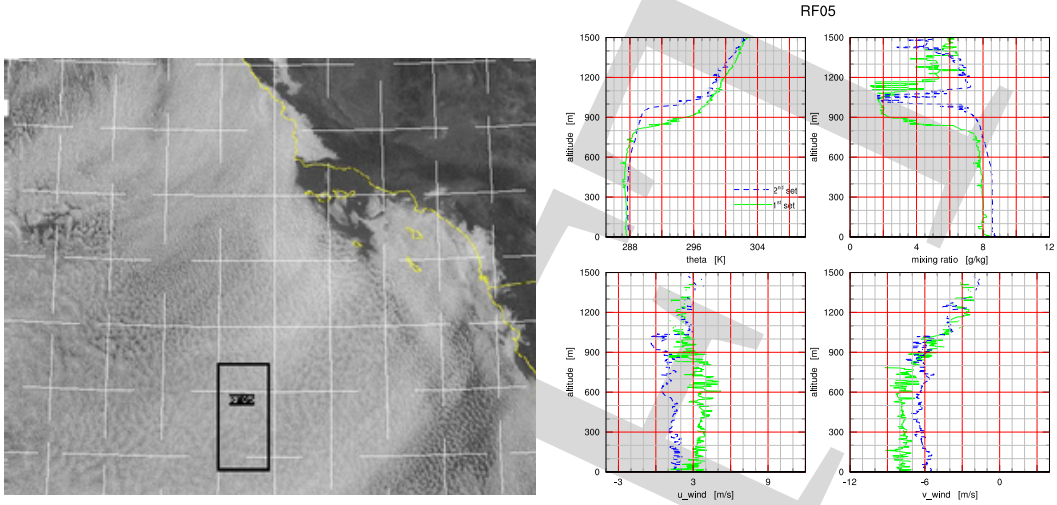

Figure 10: 1400 (UTC) cloud cover over target area and composite dropsonde data for RF05.

Table 7: RF05 offset times for flight segments

#	*GALT* [m]	*Time* [s]	Type	#	*GALT* [m]	*Time* [s]	Type
1	2578 ± 4.2	4638 - 6473	RL	1	2572-158	6478-6858	FP
2	728 ± 3.5	7412 - 10766	CB	2	158-975	6858-7068	FP
3	356 ± 3.4	11300 - 14763	SC	3	975-646	7080-7168	CP
4	1007 ± 2.4	15158 - 16808	RL	4	729-1020	10763-10830	CP
5	784 ± 3.1	17330 - 20663	CT	5	1020-154	10830-11027	FP
6	Porpoising	20656 - 22349	SP	6	154-396	11028-11088	SP
6	752 ± 4.7	22463 - 24083	CT	7	356-172	14759-14805	SP
7	100 ± 4.6	25043 - 27028	SF	8	136-1025	14824-14969	FP
8	2526 ± 4.4	27348 - 28838	RL	9	1010-736	16801-16880	IP
				10	755-108	24078-24267	FP
				11	99-2570	27023-27273	FP

cloud top.

2.6 RF06 07/20/2001 (05:39:44-15:13:00 UTC) Radar Flight

RF06 was a radar flight. The basic patterns consisted of clover-leafs and hairpins. Gabor Vali served as the mission scientist on this flight, Graham Feingold and Shouping Wang were observers. Cloud top at 800m was slightly lower than RF04 as conditions returning slowly to those of the previous week. Cloud liquid water contents were also commensurate with those of the previous week, with mixing ratios reaching 0.6 gkg^{-1} at cloud top. There was extensive drizzle observed during the flight. One focus of the flight was on the boundaries between precipitating and non-precipitating regions. There were no dropsondes on this flight and sounding legs have yet to be identified and processed.

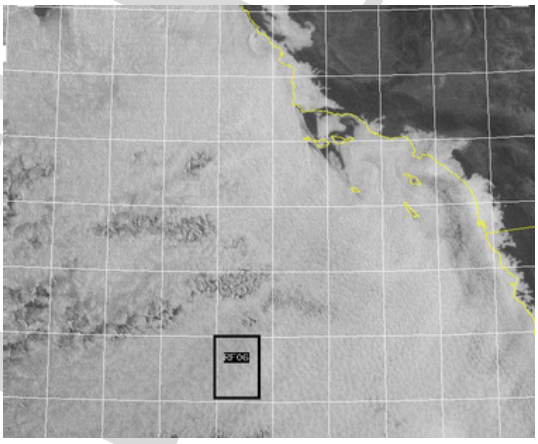

Figure 12: Satellite overview of target area for RF06

2.7 RF07 07/24/2001 (05:53:22-15:49:19)

RF07 was the last nighttime flight. The overall conditions were similar to the first week. The cloud field was very homogeneous over most of the offshore regions, the only place where there was evidence of breaks in the cloud field was in the vicinity of the target area (Fig. 13). Despite evidence of breaks (reminiscent of RF02) the cloud field appeared rather homogeneous during the flight, albeit with significant drizzle. In contrast to RF02 drizzle tended to be more uniform through the target area, and undulations at cloud top were not as pronounced.

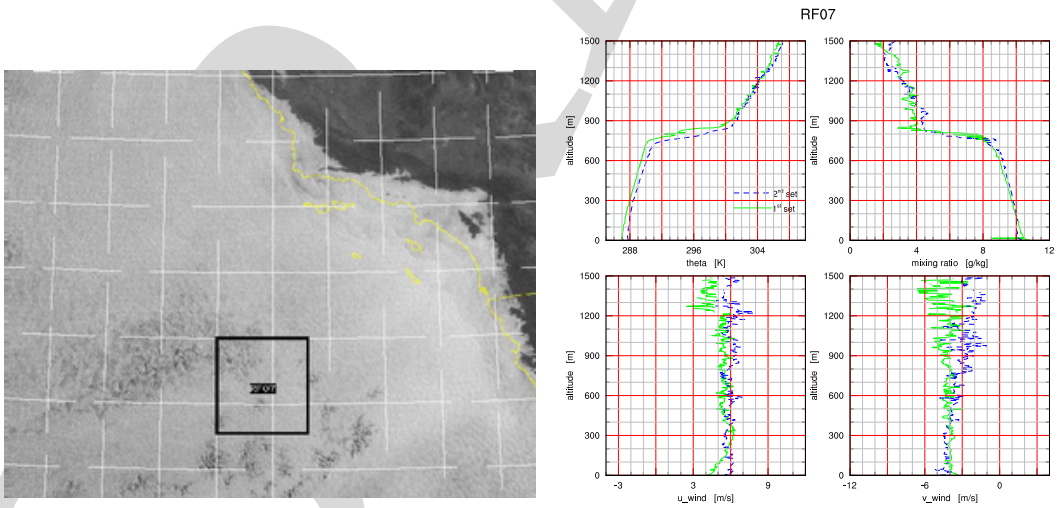

Figure 13: 1400 (UTC) cloud cover over target area and composite dropsonde data for RF07.

The dropsondes indicate that conditions in the free troposphere were both homogeneous and stationary, with somewhat moister air aloft as compared to RF01. Through the course of the experiment the boundary layer shallowed and warmed with very little change in water vapor mixing ratios. Winds were more westerly than they had been on previous flights and perhaps somewhat lighter. However their somewhat more westerly orientation kept driving us toward restricted airspace which required adjustments which took us off our initially sampled air-mass. Similar to RF04, cloud top

liquid-water mixing ratios were consistently above 0.8 gkg^{-1}. Cloud drop concentrations as indicated by the FSSP-100 were about 150 # cm^{-3} for most of the flight. CN concentrations were near 300 #cm^{-3} in the boundary layer, but considerably higher (500 #cm^{-3}) aloft.

Table 8: RF07 offset times for flight segments

#	*GALT* [m]	*Time* [s]	Type	#	*GALT* [m]	*Time* [s]	Type
1	2613 ± 2.4	7423 - 9618	RL	1	2621 - 145	9614 - 10187	FP
2	448 ± 4.9	10690 - 14440	CB	2	145 - 920	10187 - 10473	FP
3	230 ± 4.2	14770 - 18541	SC	3	921 - 426	10472 - 10680	CP
4	1070 ± 3.1	18788 - 20598	RL	4	444 - 973	14400 - 14515	CP
5	712 ± 4.4	20708 - 22588	CT	5	973 - 158	14515 - 14683	FP
6	677 ± 5.1	22598 - 24508	CT	6	144 - 1090	18563 - 18758	FP
7	Porpoising	24773 - 25718	SP	7	1071 - 706	20597 - 20728	IP
8	95 ± 6.5	25910 - 29803	SF	8	679 - 140	24501 - 24628	SP
9	2553 ± 4.1	30173 - 32050	RL	9	140 - 919	24628 - 24809	FP
				10	902 - 85	25641 - 25915	FP
				11	97 - 2564	29796 - 30127	FP

Bjorn Stevens served as mission scientist for this flight, with Verica-Savic Jovcic serving as mission specialist. Most instruments performed admirably, with the FSSP-100 functioning well for the entire flight after intermittent behavior during the second week. The porpoising leg was cut a bit short to allow a full hour at the surface. In addition an extra 30 minute cloud base leg was flown after the porpoising leg, but before the surface leg. Because of a FOD alert at North Island the airport was closed and we were forced to land at San Diego.

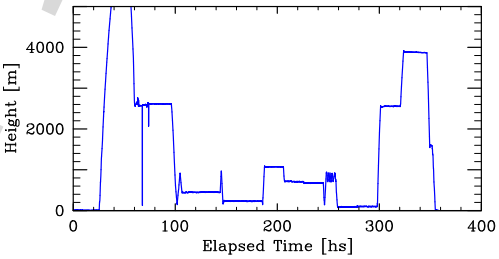

Figure 14: RF07 flight legs

2.8 RF08 07/26-27/2001 (19:45:22-05:20:34 UTC)

RF08 was the first daytime flight. It arose because the need to land at Lindbergh Field in San Diego after RF07 forced a change in schedule that was most easily accommodated by moving to a daytime schedule in anticipation of the daytime radar flight RF09 and the daytime CO_2 test-flight. Once again the cloud field was solid and homogeneous, with some evidence of the more broken, drizzle-like, structures south of the target area. Overall drizzle was very prevalent, but tended to predominate in the NE portion of the target area.

The dropsonde and aircraft data indicate a boundary layer that was shallower than on any of the previous flights. Apart from a slight moistening there was little evolution in the mean state through the course of the flight. The mean state was also very homogeneous with readily identifiable moist layers above the boundary layer. These moist layers were identifiable visibly as haze and had markedly larger CN concentrations and Ozone levels. Tracking the layer at about 1 km between the first and last set of sondes indicates a subsidence rate of about 4.5 mms^{-1} at that level, consistent with a constant divergence of 5×10^{-6} in the boundary layer. This evolution is also consistent with similar calculations based on the aircraft soundings into and out of the target

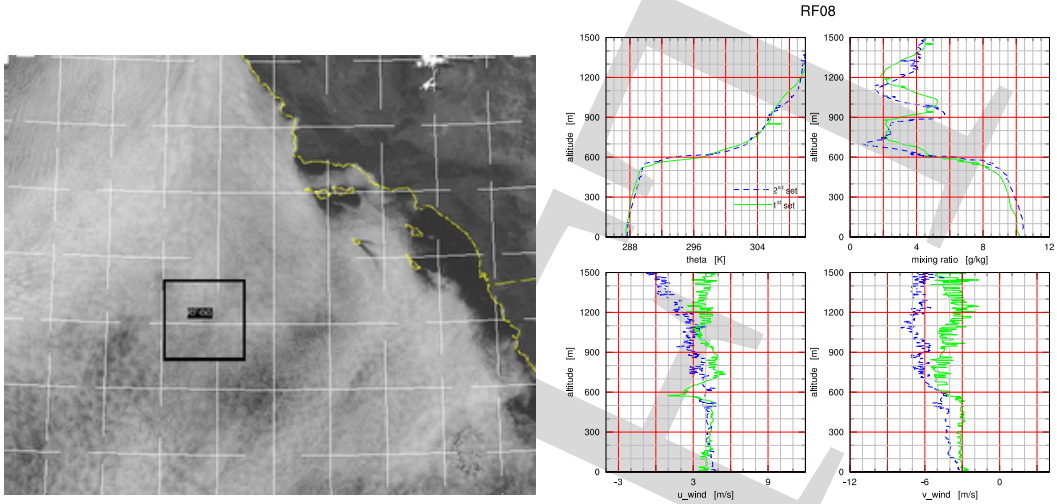

Figure 15: 1400 (UTC) cloud cover over target area and composite dropsonde data for RF08.

area. The free-troposphere was very warm aloft, with temperatures at 1km five or more Kelvin warmer than on previous flights. This is consistent with more east-west continuity in Temperature at 850 hPa than was evident during week 2. Winds on target continued to be light.

Cloud top liquid water contents were about 0.5 gkg^{-1} but cloud base was quite variable. Cloud drop concentrations were about 100 $\#cm^{-3}$. There was a marked increase of turbulence through the flight. The first part of the flight was toward mid day and the surface cloud structure was very patchy, almost scuddy (but not clearly decoupled). Turbulence on the near surface legs was very mild, and there were strong variations in visibility and surface reflectivity (indicative of more incident sunlight). On the later subcloud legs cloud base appeared much more uniform and there was a marked increase in turbulence.

Table 9: RF08 offset times for flight segments.

#	*GALT* [m]	*Time* [s]	Type	#	*GALT* [m]	*Time* [s]	Type
1	5695 ± 5.3	5839 - 7680	RL	1	5694 - 136	7675 - 8741	FP
2	437 ± 1.9	9158 - 10908	CB	2	136 - 569	8741 - 8848	FP
3	472 ± 2.2	10956 - 12824	CB	3	604 - 417	8923 - 9053	CP
4	135 ± 2.4	13184 - 14924	SF	4	467 - 640	12818 - 12908	CP
5	255 ± 2.2	15043 - 16938	SC	5	637 - 126	13003 - 13168	FP
6	1067 ± 2.9	17378 - 19058	RL	6	253 - 61	16942 - 16997	SP
7	Porpoising	19199 - 20999	SP	7	61 - 913	16997 - 17172	FP
8	90 ± 2.9	21195 - 23013	SF	8	1068 - 476	19059 - 19182	IP
9	275 ± 2.9	23273 - 24908	SC	9	542 - 94	21016 - 21177	FP
10	495 ± 2.6	25238 - 26963	CB	10	269 - 720	24903 - 25038	CP
11	524 ± 2.9	27112 - 28417	CT	11	720 - 499	25038 - 25113	IP
12	2583 ± 3.3	28838 - 32338	RL	12	526 - 185	28418 - 28485	SP
				13	185 - 2606	28485 - 28818	FP

Don Lenschow served as mission scientist and Bjorn Stevens was mission specialist. The flight track was

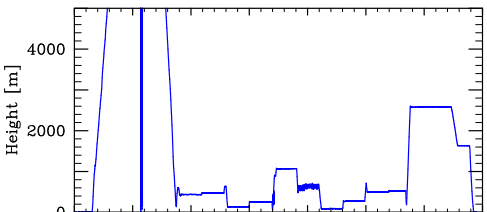

similar to the other entrainment flights except daytime conditions allowed us to intersperse the surface subcloud legs. We also made slight elevation adjustments between circles to better profile the cloud layer. Problems with the Elevator trim on the aircraft prevented us from flying particularly low surface legs, especially during the first part of the time on target when visibility was reduced due to the more patchy nature of the subcloud layer. Instruments for the most part continued to perform well.

2.9 RF09 07/27-28/2001 (19:00:00-04:00:00 UTC) Radar Flight

RF09 was the last research flight and was a daytime radar flight. The basic patterns are illustrated in Fig. 1. Gabor Vali served as the mission scientist on this flight, Verica Savic-Jovcic and David Meecham served as flight observers. Cloud top at 600m was commensurate with RF08, although the cloud layer had thinned and their was very little drizzle. Nonetheless there were sufficient radar echos to be useful. There was also increasing evidence of the haze layers that we saw for the first time on RF08. There were no dropsondes on this flight and sounding legs have yet to be identified and processed.

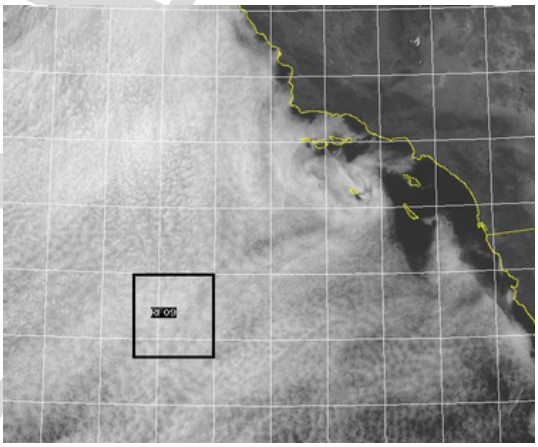

Figure 17: Satellite overview of target area for RF09

2.10 Summary

To summarize, all of the flights experienced essentially solid cloud cover. To the extent that breaks existed, these seemed to be essentially local thinnings which resulted from drizzle. While the cases did not differ in the extent of cloud cover, they did differ substantially in the amount of liquid water, the microstructure of the cloud and the thermodynamic jumps at cloud top. These differences are summarized with the help of Table 2.10. These summaries are based on preliminary RAF data and may be updated as probes are calibrated and data sources are re-evaluated. We note from the table the considerable variability in boundary layer depth, cloud microstructure and amount of drizzle.

In terms of organizing the cases for subsequent study, all of the entrainment flights excepting RF02 and RF04 are in relatively stationary environments, making them the most straight forward to study from an energetic perspective. The energetics of RF02 is complicated by the considerable variability in free tropospheric water vapor among groups of soundings, while the pronounced evolution of θ in the free troposphere in RF04 complicates its interpretation.

From the point of view of microstructure and aerosol indirect effects, the differences between RF02 and RF03 are particularly interesting. Both had relatively moist free troposphereres, yet differed substantially in terms of available CN, drop concentrations and drizzle. The possible anthropogenic origins of the RF03 aerosol, and the pronounced satellite signature should further heighten our interest. This analysis could be extended to evaluating RF07, where again pronounced drizzle seems to have a distinct satellite signature. The role of drizzle, its prevalence and apparent

Table 10: Summary of properties of cloud layer on various flights. z_i denotes the height of the lidar derived cloud top on the last lidar leg. This may have an offset associated with lidars choice for aircraft altitude. $Q_l(z_{i-})$ denotes the height of cloud top liquid water averaged over all of the FP soundings. This tends to be somewhat less than the maximum liquid water values quoted in text. Drop concentrations are derived from sounding data using the FSSP-100 on the FP soundings. CN and CCN (at 1%) are preliminary estimates derived from below cloud legs by Jeff Snider. The Max Echo is just the scale maximum chosen to best display the radar data. The thermodynamic jumps $\Delta\Theta_l$ and ΔQ_t are estimated from the sounding data.

Flight	z_i [m]	$Q_l(z_{i-})$ [gkg^{-1}]	Drops [# cm^{-3}]	CCN [#cm^{-3}]	CN [#cm^{-3}]	Max Echo [dBz]	$\Delta\Theta_l$ [K]	ΔQ_t [gkg^{-1}]
RF01	812	0.39	136	161	274	0	13	7
RF02	721	0.44	72	61	290	20	20	4-7
RF03	652	0.49	170	298	472	0	9	4-6
RF04	1060	0.67	—	207	290	10	6-12	2-6
RF05	954	0.26	170	211	417	—	9	6
RF06	—	—	—	177	389	10	—	—
RF07	795	0.75	140	139	281	10	12	6
RF08	640	0.41	100	133	245	0	12	6
RF09	—	—	—	—	-5	—	—	

regulation by condensation nuclei, some of which may be of anthropogenic origin, could be a particularly important scientific result.

3 Instruments

In this section we summarize in more detail the performance and quirks of various instruments. As an overview Table 3 indicates the status of various instruments for the nine research flights. Instrument performance is rated on a five point scale: 1 being completely down; 2 indicating intermittent functionality, 3 indicating partial functionality, 4 only minor non-functionality; 5 being perfect functionality. The behavior of some individual instruments is assessed in more detail subsequently, for PI flow instruments further information can be obtained from the instrument PI.

4 Radar Data Overview

5 Summary

Table 11: Preliminary overview of performance of key instruments for DYCOMS-II

Instrument	RF01	RF02	RF03	RF04	RF05	RF06	RF07	RF08	RF09
PVM	3	4	5	3	5	5	5	5	5
CIN	5	5	5	5	5	5	5	5	5
Fast-FSSP	1	1	5	5	5	5	4	5	5
Ultra Fast Thermometer	1	1	3	1	3	1	1	3	3
Multi-Channel Radiometer	3	3	3	3	3	3	3	4	4
FSSP-100	5	5	5	3	2	2	5	5	5
Cloud water collector	4	5	5	5	5	5	5	5	5
Stub Lyman-α	4	4	4	3	3	3	3	3	3
Cross-Flow Lyman-α	4	4	4	4	4	4	4	4	4
Ophir	1	1	1	1	1	1	1	1	1
Rosemont Thermometers	5	5	5	5	5	5	5	5	5
CVI	1	1	5	5	5	5	5	5	5
Radar	4	4	4	5	5	5	5	5	5
Lidar	4	4	4	4	4	4	4	4	4
Fast O_3	5	5	5	5	5	5	5	5	5
Slow O_3	5	5	5	5	5	5	5	5	5
CO_2	5	5	5	5	5	5	5	5	5
CO	5	5	5	5	5	5	5	5	5
TDL	3	4	4	4	1	1	4	4	4